

Linewidth enhancement factor in semiconductor lasers subject to various external optical feedback conditions

Chao-Fu Chuang,¹ Yi-Huan Liao,¹ Chih-Hao Lin,¹ Siao-Yu Chen,¹
Frédéric Grillot,² and Fan-Yi Lin^{1*}

¹*Institute of Photonics Technologies, Department of Electrical Engineering,
National Tsing Hua University, Hsinchu 30013, Taiwan*

²*Institut Mines-Télécom, Telecom ParisTech, CNRS LTCI, 46 rue Barrault, 75634 Paris
Cedex, France*

[*fylin@ee.nthu.edu.tw](mailto:fylin@ee.nthu.edu.tw)

Abstract: The linewidth enhancement factor α of a semiconductor laser under the influences of optical feedback with different feedback strengths, external cavity lengths, and feedback phases are studied both experimentally and theoretically. The value of α is determined from the minimum of the Hopf bifurcation curve when the laser is subject to both optical feedback and optical injection. In the experiment, a pellicle beamsplitter mounted on a PZT stage placed on a linear translation stage is used as the reflector, where the external cavity length can be adjusted continuously from the long cavity regime to the short cavity regime with phase accuracy. With a moderate feedback strength, α is found to increase as the feedback strength increases. Moreover, while α is insensitive to the feedback phase in the long cavity regime, it can be tuned continuously in the short cavity regime when varying the phase. A normalized variation range of 21.59% is obtained experimentally at an external cavity length of 1.5 cm, which can be further enhanced by shortening the external cavity. To the best of our knowledge, this is the first detailed study of α from the long to the short cavity regime in a semiconductor laser subject to optical feedback. More particularly, the continuous tuning of α under phase variation is demonstrated the first time.

© 2014 Optical Society of America

OCIS codes: (140.5960) Semiconductor lasers; (190.3100) Instabilities and chaos; (300.3700) Linewidth.

References and links

1. C. H. Henry, "Theory of the linewidth of semiconductor lasers," *IEEE J. Quantum Electron.* **18**, 259–264 (1982).
2. H. Li, J. Ye, and J. G. McInerney, "Detailed analysis of coherence collapse in semiconductor lasers," *IEEE J. Quantum Electron.* **29**, 2421–2432 (1993).
3. T. Zhang, N. H. Zhu, B. H. Zhang, and X. Zhang, "Measurement of chirp parameter and modulation index of a semiconductor laser based on optical spectrum analysis," *IEEE Photon. Technol. Lett.* **19**, 227–229 (2007).
4. M. Osinski and J. Buus, "Linewidth broadening factor in semiconductor lasers—An overview," *IEEE J. Quantum Electron.* **23**, 9–29 (1987).
5. U. Kruger and K. Kruger, "Simultaneous measurement of the linewidth enhancement factor α , and FM and AM response of a semiconductor laser," *J. Lightwave Technol.* **13**, 592–597 (1995).
6. J. G. Provost and F. Grillot, "Measuring the Chirp and the Linewidth Enhancement Factor of Optoelectronic Devices with a Mach-Zehnder Interferometer," *IEEE Photon. J.* **3**, 476–488 (2011).
7. C. H. Lin, H. H. Lin, and F. Y. Lin, "Four-wave mixing analysis of quantum dot semiconductor lasers for linewidth enhancement factor extraction," *Opt. Express* **20**, 101–110 (2012).

8. K. E. Chlouverakis, K. M. Al-Aswad, I. D. Henning, and M. J. Adams, "Determining laser linewidth parameter from Hopf bifurcation minimum in lasers subject to optical injection," *Electron. Lett.* **39**, 1185–1187 (2003).
9. Y. Yu, G. Giuliani, and S. Donati, "Measurement of the linewidth enhancement factor of a semiconductor laser based on the optical feedback self-mixing effect," *IEEE Photon. Technol. Lett.* **16**, 1185–1187 (2004).
10. G. P. Agrawal and C. M. Bowden, "Concept of linewidth enhancement factor in semiconductor lasers: Its usefulness and limitations," *IEEE Photon. Technol. Lett.* **5**, 227–229 (1993).
11. R. J. Jones, P. S. Spencer, J. Lawrence, and D. M. Kane, "Influence of external cavity length on the coherence collapse regime in laser diodes subject to optical feedback," *IEE Proc. Optoelectron.* **148**, 7–12 (2001).
12. B. Lingnau, K. Lüdge, W. W. Chow, and E. SchÖll, "Failure of the α factor in describing dynamical instabilities and chaos in quantum-dot lasers," *Phys. Rev. E* **86**, 065201 (2012).
13. C. H. Lin and F. Y. Lin, "Four-wave mixing analysis on injection-locked quantum dot semiconductor lasers," *Opt. Express* **21**, 21242–21253 (2013).
14. Y. Yu and J. Xi, "Influence of external optical feedback on the alpha factor of semiconductor lasers," *Opt. Lett.* **38**, 1781–1783 (2013).
15. K. Kechaoou, F. Grillot, J. G. Provost, B. Thedrez, and D. Erasme, "Self-injected semiconductor distributed feedback lasers for frequency chirp stabilization," *Opt. Express* **20**, 26062–26074 (2012).
16. A. Gavrielides, V. Kovani, and T. Erneux, "Analytical stability boundaries for a semiconductor laser subject to optical injection," *Opt. Commun.* **136**, 253–256, (1997).
17. F. Y. Lin and J. M. Liu, "Nonlinear dynamical characteristics of an optically injected semiconductor laser subject to optoelectronic feedback," *Opt. Commun.* **221**, 173–180, (2003).
18. D. Lenstra, B. H. Verbeek, and A. J. D. Boef, "Coherence collapse in single-Mode semiconductor lasers due to optical feedback," *IEEE J. Quantum Electron.* **21**, 674–679 (1985).
19. F. Grillot, B. Dagens, J. G. Provost, H. Su, and L. F. Lester, "Gain compression and above-threshold linewidth enhancement factor in 1.3-um InAs-GaAs quantum-dot lasers," *IEEE J. Quantum Electron.* **44**, 946–951 (2008).

1. Introduction

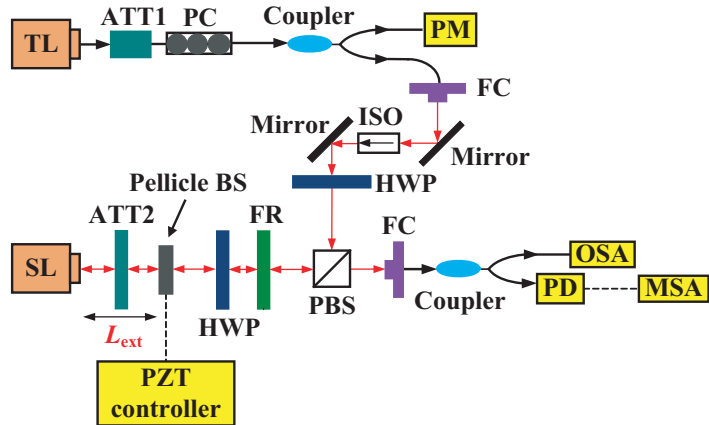
The linewidth enhancement factor α is one of the fundamental parameters for semiconductor lasers. It is also named as the α parameter, the Henry factor, the chirp factor, or the phase-amplitude coupling factor, which determines important laser characteristics including stability [1], coherence collapse [2], chirp [3], and modulation response [4]. Various techniques, such as the AM/FM method with current modulation [5, 6], the four-wave mixing and the Hopf bifurcation minimum methods with optical injection [7, 8], and the self-mixing method with optical feedback [9], have commonly been employed to measure the α .

In many theoretical models, α has been set as a constant parameter independent of the operation conditions [10, 11]. However, with optical injection, α has been shown to vary with different injection strengths and detuning frequencies [12, 13]. With optical feedback, α has been shown to increase with the feedback strength in the long cavity regime [14]. With a relatively weak feedback, reduction in α from its free-running value has also been observed [15]. While the effects from the external feedback are determined not only by the feedback strength but also by the external cavity length and the feedback phase, it is of great interest to study the α of semiconductor laser subject to various external optical feedback conditions.

In this paper, we investigate the variations of α from the long cavity regime to the short cavity regime with different feedback strengths, external cavity lengths, and feedback phases. To the best of our knowledge, the continuous variation of the α under different feedback phases is shown for the first time. Moreover, by varying the feedback phase in the short cavity regime, enhancement and reduction of the α tuned away from its free-running value are demonstrated.

2. Schematic setup

A Hopf bifurcation minimum method is used to measure the α , which determines α from the turning point (minimum detuning frequency f_{\min}) of the Hopf bifurcation curve [8]. By optically injecting the laser, the Hopf bifurcation curve corresponding to the upper detuning frequency boundary of the stable locking region can be obtained. From the normalized minimum detuning frequency of the Hopf bifurcation curve ω_{\min} (f_{\min} normalized to the relaxation



TL: Tunable laser
SL: Semiconductor laser
ATT1, 2: Attenuator1, 2
PC: Polarization controller
FC: Fiber coupler
ISO: Isolatter
HWP: Half-wave plate

PBS: Polarizing beamsplitter
FR: Faraday rotator
Pellicle BS: Pellicle beamsplitter
PM: Power meter
PD: Photo detector
OSA: Optical spectrum analyzer
MSA: Microwave spectrum analyzer

Fig. 1. Experimental setup for measuring the α of a semiconductor laser subject to various feedback conditions.

oscillation frequency f_r), α can be approximated using [8]

$$\omega_{\min} \simeq -\sqrt{\frac{(\alpha^2 - 1)^3}{32\alpha^2}}. \quad (1)$$

This approximation is valid under the conditions that (1) the electron lifetime is much greater than the photon lifetime, (2) the reciprocal of $|f|$ (f is the detuning frequency between the TL and the SL) is much larger than the photon lifetime, and (3) $\alpha > 1$ [16].

In this study, the variations of α under different feedback conditions are studied both experimentally and numerically. Figure 1 shows the experimental setup for measuring the α of a semiconductor laser subject to optical feedback. The laser under test is a single-mode distributed-feedback (DFB) semiconductor laser (SL) biased at 20 mA ($2.5I_{th}$). The wavelength of the SL at free-running is 1529.6 nm. To determine α , the SL is optically injected by a tunable laser (TL) (Yenista Tunics-T100S, tuning range of 100 nm) through a free space circulator. By sweeping the detuning frequency f (the frequency difference of the TL and the SL) at different normalized injection strengths ξ_i (the injection field normalized to the SL output field), the minimum detuning frequency of the Hopf bifurcation curve f_{\min} can be obtained and α can be calculated using Eq. (1). To investigate the influence of the optical feedback, α at different feedback strengths η_{fb} , external cavity lengths L_{ext} , and feedback phases ϕ_{fb} are measured. Here the feedback is provided by a pellicle beamsplitter with a reflectivity of 8%, which is placed on a PZT carried by a linear translation stage. The feedback strength η_{fb} (the feedback field, before coupling into the SL, normalized to the SL output field) is controlled by a variable attenuator (ATT2). The L_{ext} is adjusted by the translation stage while the ϕ_{fb} is fine tuned by the PZT. In this setup, the L_{ext} can be continuously varied from the long cavity regime to the short

cavity regime, where their boundary is at about $L_{\text{ext}} = 3.66$ cm corresponding to a relaxation oscillation frequency of $f_r = 4.1$ GHz. The output of the SL is monitored and analyzed with an optical spectrum analyzer (Advantest Q8384) and a microwave spectrum analyzer (Agilent E4407B).

3. Simulation model

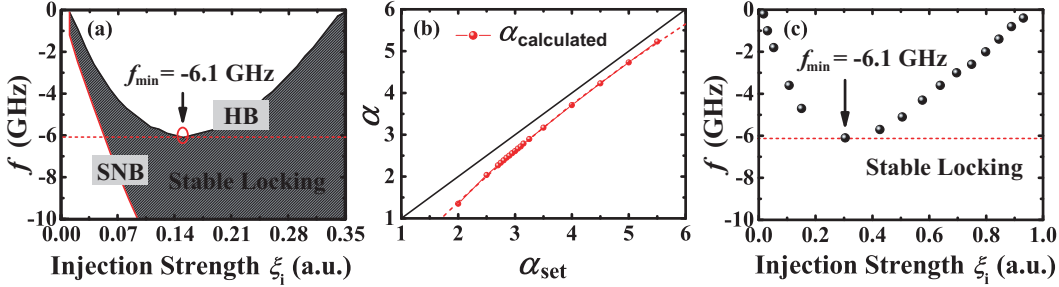


Fig. 2. (a) Stability map obtained numerically with Eqs. (2)-(4) using the laser parameters extracted. HB: Hopf bifurcation; SNB: saddle-node bifurcation. (b) α calculated from the Hopf bifurcation minimum by using Eq. (1). (c) Hopf bifurcation curve obtained experimentally with the optically-injected SL.

In simulation, the dynamics of a semiconductor laser subject to both optical injection and optical feedback can be described by the rate equations of the normalized optical field a , the optical phase ϕ , and the normalized carrier density n [17]:

$$\begin{aligned} \frac{da}{dt} &= \frac{1}{2} \left[\frac{\gamma_c \gamma_n}{\gamma_s J} n - \gamma_p (2a + a^2) \right] (1 + a) \\ &\quad + \xi_i \gamma_c \cos \phi \\ &\quad + \xi_{\text{fb}} \gamma_c [1 + a(t - \tau)] \cos[\phi(t - \tau) - \phi(t) + \phi_{\text{fb}}], \end{aligned} \quad (2)$$

$$\begin{aligned} \frac{d\phi}{dt} &= -\frac{\alpha_{\text{set}}}{2} \left[\frac{\gamma_c \gamma_n}{\gamma_s J} n - \gamma_p (2a + a^2) \right] \\ &\quad - \frac{\xi_i \gamma_c}{1 + a} \sin \phi + 2\pi f \\ &\quad + \xi_{\text{fb}} \gamma_c \frac{[1 + a(t - \tau)]}{1 + a} \sin[\phi(t - \tau) - \phi(t) + \phi_{\text{fb}}], \end{aligned} \quad (3)$$

$$\begin{aligned} \frac{dn}{dt} &= -\gamma_s n - \gamma_n (1 + a)^2 n - \gamma_s J (2a + a^2) \\ &\quad + \frac{\gamma_s \gamma_p}{\gamma_c} J (2a + a^2) (1 + a)^2, \end{aligned} \quad (4)$$

where J is the normalized dimensionless injection current parameter, γ_c is the cavity decay rate, γ_s is the spontaneous carrier relaxation rate, γ_n is the differential carrier relaxation rate, γ_p is the nonlinear carrier relaxation rate, α_{set} is the linewidth enhancement factor set in the rate equation model, ξ_i and f are the normalized optical injection strength and detuning frequency, ξ_{fb} is the normalized optical feedback strength, ϕ_{fb} is the optical feedback phase, and $\tau = 2L_{\text{ext}}/c$ is the feedback delay time [17]. To better coincide with the experimental results, a four-wave mixing analysis is employed to extract the laser parameters of the SL used in the experiment [7]. At

$J = 1.35$, $\gamma_c = 2.31 \times 10^{11} s^{-1}$, $\gamma_s = 5.93 \times 10^9 s^{-1}$, $\gamma_n = 2.87 \times 10^9 s^{-1}$, $\gamma_p = 1.35 \times 10^{11} s^{-1}$, and $\alpha_0 = 3.46$ (α at free-running) are obtained. The values of the electron lifetime ($1/\gamma_s$), photon lifetime ($1/\gamma_c$), and α satisfy the conditions of the approximation used in Eq. (1).

To check the accuracy of the approximation of Eq. (1) for the SL under test, Fig. 2(a) shows the stability map obtained numerically with Eqs. (2)-(4) using the laser parameters extracted. As can be seen, by setting an $\alpha_{\text{set}} = 3.46$ in the simulation, a f_{\min} at -6.1 GHz is obtained and a corresponding α of 3.14 is calculated by using Eq. (1). For different α_{set} set between 2 to 5.5, the α calculated are plotted in Fig. 1(b)(red dots). Although fairly close, the α calculated with Eq. (1) is slightly lower than which it is supposed to be (the black line denotes the α_{set} set in the simulation) for the SL used in our experiment. By fitting the calculated α (red dashed curve), α in this study will be adjusted with

$$\alpha(\text{adjust}) = 0.039\alpha^2 + 0.655\alpha + 1.02 \quad (5)$$

to reduce the discrepancy and better describe the property of the SL.

This adjustment is verified experimentally, where Fig. 2(c) shows the Hopf bifurcation curve of the optically-injected SL. A $f_{\min} = -6.1$ GHz is obtained and, from Eqs. (1) and (5), an $\alpha = 3.46$ is calculated. The value of the α agrees well with the value independently extracted from the four-wave mixing analysis.

4. Results and discussion

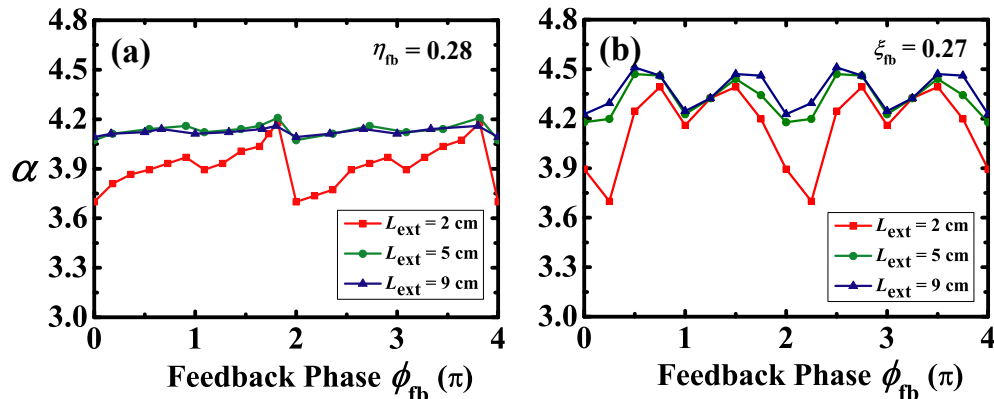


Fig. 3. Phase variations of α obtained (a) experimentally with $\eta_{\text{fb}} = 0.28$ and (b) numerically with $\xi_{\text{fb}} = 0.27$ for $L_{\text{ext}} = 2 \text{ cm}$, 5 cm, and 9 cm, respectively.

To show the influence of the feedback delay on α , Fig. 3(a) depicts the variations of α for different ϕ_{fb} with $\eta_{\text{fb}} = 0.28$ and $L_{\text{ext}} = 2 \text{ cm}$, 5 cm, and 9 cm. As can be seen, with $L_{\text{ext}} = 9 \text{ cm}$ in the long cavity regime, α is almost insensitive to the ϕ_{fb} . As the L_{ext} gets shorter, α becomes phase sensitive and varies continuously in a cycle of 2π . For $L_{\text{ext}} = 2 \text{ cm}$ which falls in the short cavity regime, α varies notably from 3.7 to 4.18 for different ϕ_{fb} . Similar behaviors are found in simulation, where Fig. 3(b) shows the phase variation of α with $\xi_{\text{fb}} = 0.27$. As L_{ext} is shortened from 9 cm to 2 cm, the ranges of variation gradually become larger. With $L_{\text{ext}} = 2 \text{ cm}$ in the short cavity regime, as shown in Figs. 3(a) and 3(b), normalized variation ranges (normalized to α_0) of 13.86% and 20.02% are measured experimentally and numerically. Note that, the variation in the SL output power (or the effective pump level) due to optical feedback may also lead to the change in f_{\min} and affect the accuracy of Eq. (1) in determining α [16]. However, even for the conditions of $\eta_{\text{fb}} = 0.28$ and $L_{\text{ext}} = 2 \text{ cm}$, the variation of the SL output power in

our setup is only $20\mu\text{W}$ when varying ϕ_{fb} (compared to a power of 1.632 mW at free-running). From the calculation, the possible deviation in α due to the change in the effective pump level is less than 0.01, which is much smaller than the variations that we have observed and can therefore be ignored.

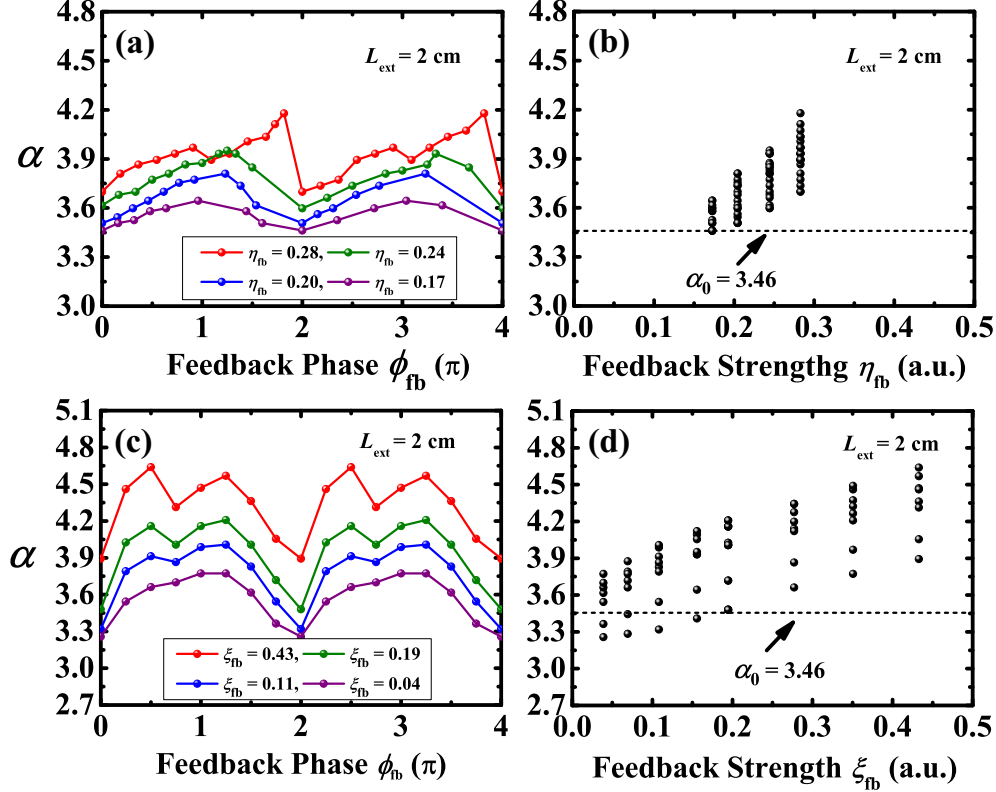


Fig. 4. Phase variations of α obtained (a) experimentally and (c) numerically for different η_{fb} and ξ_{fb} , respectively. To show the variation ranges, α covering a range of 4π (two cycles) are plotted for different (b) η_{fb} and (d) ξ_{fb} . Here L_{ext} is 2 cm in the short cavity regime. The dashed lines indicate the α at free-running.

Figure 4(a) shows the phase variations of α experimentally obtained in the short cavity regime with $L_{\text{ext}}=2\text{ cm}$ for different η_{fb} . For each η_{fb} , α covering a range of 4π (two cycles) are plotted in Fig. 4(b) to show the variation ranges. As can be seen, as η_{fb} increases, both α and its variation range increase. With a moderate feedback level applied ($\eta_{\text{fb}}=0.17 \sim 0.28$), the relaxation oscillation becomes undamped and the laser linewidth gets broadened in this region [18]. Note that, while α below its free-running value (the dashed line) can be obtained for $\eta_{\text{fb}} < 0.17$ by further attenuating the feedback light from the pellicle beamsplitter with the attenuator (ATT2), the output light from the SL will also be attenuated and becomes too weak to resolve in the current setup. Figures 4(c) and 4(d) show the phase variations and the variation ranges of α obtained numerically under different ξ_{fb} with $L_{\text{ext}}=2\text{ cm}$. Similar trend is found when ξ_{fb} increases from 0.04 to 0.43, where α and its variation range increase as ξ_{fb} increases. Note that, with a relatively weak feedback ($\xi_{\text{fb}} < 0.11$), α suppressed below its free-running value (dashed line in Fig. 4(d)) can be achieved. To the best of our knowledge, manipulating α of a semiconductor laser with optical feedback in the short cavity regime, especially the tuning of α by changing the feedback phase, is demonstrated for the first time. In practice, chirp

control in integrated devices such as the multi-section semiconductor lasers can therefore be realized by employing a phase control unit. With a sub-centimeter cavity, a much wider variation range of α is expected.

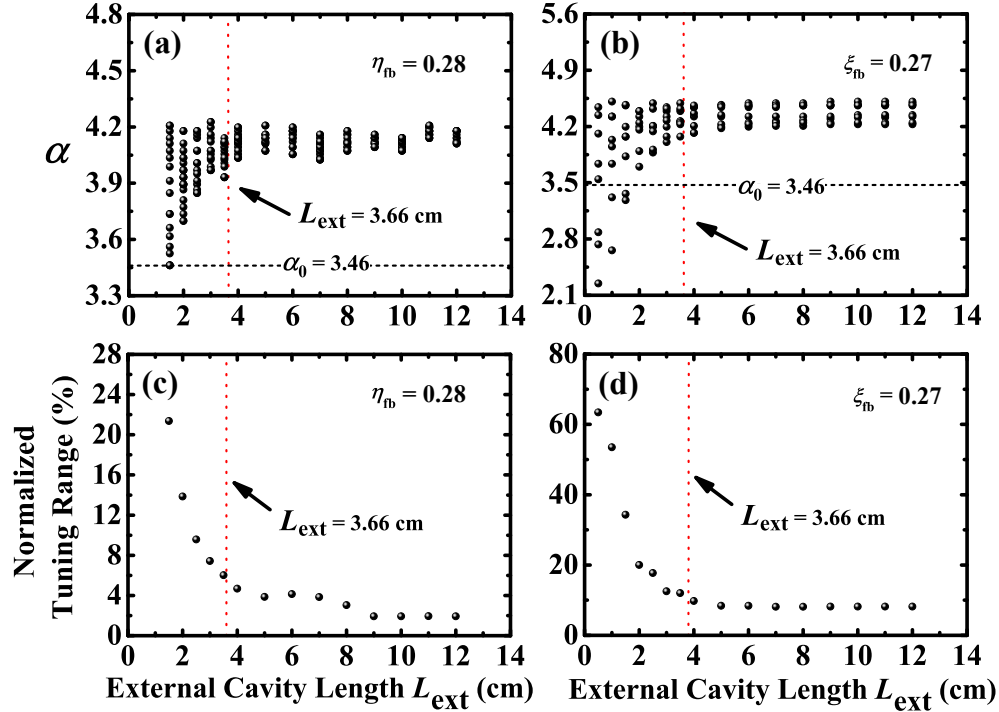


Fig. 5. (a) and (b) show α covering a range of 4π (two cycles) for different external cavity length obtained experimentally and numerically with $\eta_{\text{fb}} = 0.28$ and $\xi_{\text{fb}} = 0.27$, respectively. (c) and (d) show the respective normalized tuning ranges of α shown in (a) and (b). The red dashed lines indicate the boundary of the long and short cavity regime.

Figures 5(a) and 5(b) show α with different external cavity lengths obtained experimentally and numerically with $\eta_{\text{fb}} = 0.28$ and $\xi_{\text{fb}} = 0.27$, respectively. For each L_{ext} , α covering a range of 4π (two cycles) are plotted to show their variation ranges. For $L_{\text{ext}} > 3.66 \text{ cm}$ in the long cavity regime, as shown in Figs. 5(a) and 5(b), α are not very sensitive to the feedback phase and have average values around 4.15 and 4.35, respectively. In contrast, when L_{ext} is shortened to the short cavity regime ($L_{\text{ext}} < 3.66 \text{ cm}$), α is strongly influenced by the feedback phase and can be varied in a much wider range. While a wider tuning range is expected for a shorter L_{ext} in the experiment, however, it is difficult to have a sub-centimeter L_{ext} with the current setup. Figures 5(c) and 5(d) show the normalized variation ranges obtained experimentally and numerically with $\eta_{\text{fb}} = 0.28$ and $\xi_{\text{fb}} = 0.27$, respectively. As can be seen, the variation range increases rapidly in the short cavity regime as L_{ext} is shortened. For L_{ext} as short as 1.5 cm, a normalized variation range of 21.59% is achieved experimentally. With $L_{\text{ext}} = 0.5 \text{ cm}$, a normalized variation range of 63.41% is predicted with the simulation shown in Fig. 5(d). In such condition, as seen in Fig. 5(b), α as low as 2.25 can be obtained.

In the simulation, α suppressed below its free-running value can be achieved with relatively low reflectivity and short external cavity as shown in Figs. 4(d) and 5(b), respectively. To demonstrate α suppressed below its free-running value experimentally, Fig. 6 shows the variation of α obtained with the lowest $\eta_{\text{fb}} = 0.17$ and the shortest $L_{\text{ext}} = 1.0 \text{ cm}$ achievable in the

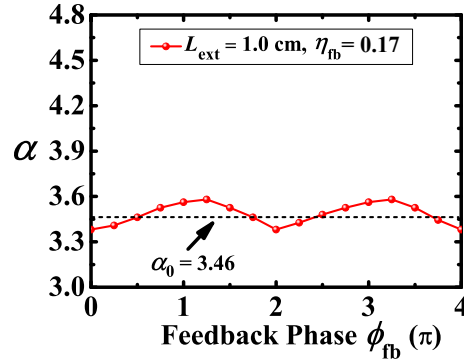


Fig. 6. α obtained experimentally with $\eta_{\text{fb}} = 0.17$ and $L_{\text{ext}} = 1.0$ cm, where α suppressed below its free-running value is demonstrated.

current setup. As can be seen, when varying the ϕ_{fb} , α dropped below its free-running value is demonstrated. To further lower α , integrating a phase control unit to shorten L_{ext} is required.

5. Conclusions

In conclusion, we study the variation of the linewidth enhancement factor α for a semiconductor laser subject to optical feedback and show a way of controlling it. By monitoring the turning point of the Hopf bifurcation curve at its minimum detuning with optical injection, α of the semiconductor laser under different feedback conditions are measured. The influences of the feedback strength, external cavity length, and feedback phase are examined. For both the long cavity and short cavity regimes, α is found to increase with the feedback strength in the moderate feedback region chosen due to the undamped relaxation oscillation. Moreover, while it is shown to be phase insensitive in the long cavity regime, it can be tuned continuously in the short cavity regime by varying the feedback phase.

The phenomenon demonstrated in this paper can be useful in controlling the chirp of an integrated compact device with the aid of phase control. From the simulation results, a wide tuning range of α is expected with an external cavity in the millimeter or sub-millimeter range. While α for different quantum-dot semiconductor lasers studied vary in a much larger range compared to the quantum-well ones [19], α of the quantum-dot semiconductor lasers subject to various optical feedback conditions will be further investigated.

Acknowledgments

This work is supported by the National Science Council of Taiwan under contract NSC-100-2112-M-007-012-MY3 and National Tsing Hua University under grant 102N7081E1.